Journal of Statistical Physics, Vol. 69, Nos. 3/4, 1992

A Stochastic Lattice Gas for Burgers' Equation: A Practical Study

Leesa Brieger[1] **and Ernesto Bonomi**[1]

Received September 5, 1991; final May 13, 1992

We continue our investigation of stochastic lattice gases as a (highly parallel) means of simulating given PDEs, in this case Burgers' equation in one dimension. The lattice dynamics consists of stochastic unidirectional particle displacement, and our attention is turned toward the reliability of the model, i.e., its ability to reproduce the unique physical solution of Burgers' equation. Lattice gas results are discussed and compared against finite-difference calculations and exact solutions in examples which include shocks and rarefaction waves.

KEY WORDS: Lattice gas; cellular automata; Monte Carlo method; parallel algorithm; Burgers' equation.

1. INTRODUCTION

In this article we investigate a lattice gas model for simulating Burgers' equation[1-3] of diffusion with nonlinear advection in one dimension,

$$u_t = \mu u_{xx} - u u_x, \qquad \mu \geqslant 0 \tag{1}$$

in which μ is a constant which determines the amount of dissipation present. This equation is generally taken as a description of the velocity of a fluid in unidimensional flow, in a simple formulation of the competition between convection and diffusion. Its solutions can form shocks, and in fact this equation realistically describes the phenomenon of the sonic boom.

The current approach is exactly that used in our prior lattice gas investigations of diffusion and reaction, only now with transition rules appropriate to the equation given above. The rules define the dynamics of

[1] CFD/MPC Project, IMHEF Ecole Polytechnique Fédérale de Lausanne, C.P. 123, CH-1015 Lausanne, Switzerland.

0022-4715/92/1100-0837$06.50/0

a population of particles on the nodes of the lattice. There are no velocities implemented in our models, and the principle of exclusion imposes the constraint of at most one particle per lattice site: each node is either occupied or free. The behavior of the occupation probabilities is described in the equations of balance (master equations) which follow from the transition rules of the automaton and describe the macroscopic evolution of the model. Under appropriate conditions, particle distribution observed in the automaton directly approximates the solution of the balance equations and furnishes the basis of the simulation.

It is worth noting here that for the viscous form ($\mu \neq 0$) of Burgers' equation, the transformation $u = -(2\mu/\theta)(\partial\theta/\partial x)$ relates $u(x, t)$ and $\theta(x, t)$ such that if θ is a solution of the linear diffusion equation $\theta_t = \mu\theta_{xx}$, then u is a solution of the viscid Burgers' equation (1), and conversely, apart from a multiplicative factor in θ which does not influence u.[4] This transformation was discovered independently by Cole, Hopf, and Burgers himself right around 1950 and furnishes a means of constructing exact solutions to the viscid Burgers' equation. Thus we are able to compare simulation results to exact solutions and accurately judge the capacity of the lattice gas model to capture the physics contained in Burgers' equation. All comparisons in this article are based on exact solutions provided by Benton and Platzman in their 1972 survey of the Burgers' equation literature.[4]

In Section 2, we detail our approach to stochastic lattice gases in general. The lattice model for Burgers' equation is defined in Section 3. An approximate master equation is derived and the correspondence between it and a finite-difference discretization of Burgers' equation is demonstrated. In Section 4 we consider nonunicity of the solution of Burgers' inviscid equation and the entropy condition in order to investigate the behavior of the model and of the master equation. In Section 5 we continue the quest for quantitative agreement between the lattice model and the exact solution in cases of front propagation.

2. GENERAL DESCRIPTION OF THE METHOD

In this section we consider the master equations which lead to a description of the ordered macroscopic behavior of the occupation probabilities in the lattice model. Depending on the transition rules of the lattice gas, these are nothing other than finite-difference equations for the continuous equations that we want to simulate.

Imagine a population of identical particles located on the nodes of a lattice and changing position according to some prescribed stochastic transition rule. An exclusion principle of at most one particle per lattice site

means that each site is completely characterized by whether or not it contains a particle. Let x_r^n be the stochastic variable which indicates the state of site r at moment n:

$$x_r^n = \begin{cases} 0 & \text{site } r \text{ is not occupied at moment } n \\ 1 & \text{site } r \text{ is occupied at moment } n \end{cases}$$

Because this is a Boolean variable, its average occupation number is given by the probability P_r^n with which $x_r^n = 1$.

In order to derive the balance equation of this model and so describe the evolution of P_r^n, we consider probabilities of transition: the probability of a particle transition from site q to site r at timestep n is given by $P_q^n W_{qr}^n$, where W_{qr}^n is the conditional probability of transition from q to r at timestep n, given a particle present at site q at this moment.

The probability P_r^{n+1} of finding a particle at site r at moment $n+1$ is just the probability that a particle transition to site r has occurred in the current timestep, including the possible "transition" from r to r. If the transition rule allows for particle displacement only between nearest neighbors on the lattice and respects the aforementioned exclusion principle, then the balance equation is determined by the probabilities of the (mutually exclusive) transitions to r from the neighboring sites as follows:

$$P_r^{n+1} = \sum_{q \in \mathcal{N}(r)} P_q^n W_{qr}^n \tag{2}$$

where $\mathcal{N}(r)$ is the neighborhood of r, composed of r itself and its nearest neighbors on the lattice.

Assuming conservation of mass in the model, we see that

$$\sum_{s \in \mathcal{N}(r)} W_{rs}^n = 1 \tag{3}$$

that is, from a site r a particle must transit to *one* of the sites in its neighborhood. We may solve (3) for W_{rr}^n, and with this rewrite the balance equation as the following evolution equation:

$$P_r^{n+1} - P_r^n = \sum_{\substack{q \in \mathcal{N}(r) \\ q \neq r}} P_q^n W_{qr} - P_r^n \sum_{\substack{q \in \mathcal{N}(r) \\ q \neq r}} W_{rq}^n \tag{4}$$

Equation (4) furnishes a deterministic description of the behavior of the occupation probabilities.

A simple example of a stochastic lattice gas such as described above consists of a solitary particle in a random walk on a square lattice. This is a well-known model of diffusion[5] which we consider to illustrate our

approach. With the random walk rule driving the particle movement on the square lattice, $W_{qr}^n = 1/4$ whenever q and r are nearest neighbors, $q \neq r$. Thus, Eq. (4), the description of the occupation probabilities, becomes

$$P_r^{n+1} - P_r^n = \tfrac{1}{4}\left(\sum_{\substack{q \in \mathcal{N}(r) \\ q \neq r}} P_q^n - 4P_r^n \right) \tag{5}$$

which is exactly the finite-difference form of the diffusion equation $u_t = D\,\Delta u$ with $D = \Delta x^2/4\,\Delta t$.

This illustrates how a particle's random walk simulates diffusive behavior: the behavior of the particle averaged over the ensemble of all realizations of its random walk reproduces the solution of the difference equation which approximates and is consistent with the continuous equation of diffusion.

The very simple methodology of this example is applicable to other lattice gases. Clearly, changing the model's transition rules will have an effect on Eq. (4) via the corresponding changes in the transition probabilities W_{qr}^n. The resulting equation may resemble the finite-difference form of another PDE, and the occupation probabilities in the lattice gas will approximate the solution of the corresponding difference equation. For example, with the appropriate bias in the random walk transition rule for a population of particles, the lattice gas simulates the nonlinear diffusion equation for a diffusion coefficient which is an arbitrary given function of the solution.[6] Transition rules which mimic chemical reactions between diffusing species will simulate reaction-diffusion equations.[7] In the present article we adapt the transition rules to simulate Burgers' equation.

3. BURGERS' EQUATION—THE MODEL

In this section we apply the above approach to a lattice gas tailored to Burgers' equation. We will be studying Burgers' equation in one dimension, so consider now a one-dimensional regular lattice upon which our population of particles will "walk." The rule that we consider is the following: each particle takes a stochastic walk to the right, respecting the exclusion principle of at most one particle per site. We use a parameter α, $0 \leqslant \alpha \leqslant 1$, to define the probability of each particle's displacement to the right: each particle chooses, with probability α, to walk to the right or, with probability $1 - \alpha$, not to move. The exclusion principle is implemented in the following way: a particle having chosen to move to the right is blocked from all action if the site to its right is already occupied. Thus the rule, applied independently and simultaneously at all sites, can be described

as follows: a particle at a site j at moment n will move with probability α to site $j+1$ at moment $n+1$ *unless* site $j+1$ is already occupied at moment n, in which case the particle at j remains stationary for this timestep.

To determine the balance equation for this simple rule, we follow the procedure and terminology of Section 2, examining the occupation probabilities P_j^n and how they evolve in time. Once again, a site j can be occupied at moment $n+1$ only if a particle transition to j, including the possible "transition" from j to j, has occurred in the preceding moment. Thus, Eq. (2) is the equation of balance for the model and, in this one-dimensional case, looks like

$$P_j^{n+1} = \sum_{k=j-1}^{j+1} P_k^n W_{kj}^n \tag{6}$$

According to the rule described above which drives the dynamics of this model and with the simplifying assumption that the occupation probabilities for different sites are independent,[8] the probabilities of transition can be written as

$$W_{k-1,k}^n = \alpha(1-P_k^n), \qquad W_{k,k}^n = \alpha P_{k+1}^n + (1-\alpha), \qquad W_{k+1,k}^n = 0 \tag{7}$$

Notice that this amounts to approximating $W_{k-1,k}^n$ and $W_{k,k}^n$ in terms of ordinary rather than conditional probabilities. In this case the balance equation (6) looks like

$$P_j^{n+1} = \alpha P_{j-1}^n (1-P_j^n) + (1-\alpha) P_j^n + \alpha P_j^n P_{j+1}^n \tag{8}$$

or, equivalently,

$$P_j^{n+1} - P_j^n = \frac{\alpha}{2}(P_{j+1}^n - 2P_j^n + P_{j-1}^n) + \frac{\alpha}{2}(2P_j^n - 1)(P_{j+1}^n - P_{j-1}^n) \tag{9}$$

With the change of variable $v_j^n = (-2P_j^n + 1)\, V$, where V is a characteristic velocity, the equation can be rewritten once again, this time as

$$v_j^{n+1} - v_j^n = \frac{\alpha}{2}(v_{j+1}^n - 2v_j^n + v_{j-1}^n) - \frac{\alpha}{2V} v_j^n (v_{j+1}^n - v_{j-1}^n) \tag{10}$$

Now consider the discretization of Burgers' equation (1), by finite differences:

$$\frac{u_j^{n+1} - u_j^n}{\Delta t} = \mu \frac{u_{j+1}^n - 2u_j^n + u_{j-1}^n}{\Delta x^2} - u_j^n \frac{u_{j+1}^n - u_{j-1}^n}{2\,\Delta x} \tag{11}$$

Under the conditions

$$\begin{cases} \alpha \dfrac{\Delta x^2}{2\,\Delta t} = \mu \\ \dfrac{\Delta t}{\Delta x} = \dfrac{\alpha}{V} \end{cases} \tag{12}$$

Eqs. (10) and (11) are exactly the same, i.e., the finite-difference form for Burgers' equation *is* our approximate balance equation, in terms of v, of the lattice gas model. Thus the occupation probabilities in the lattice gas will approximate the solution of the finite-difference equation with the discretization fixed by (12). Remark also that under the constraints of (12), the condition for linear stability for diffusion[9] as well as the Courant–Friderichs–Lewy (CFL) condition[10] are both satisfied.

A configuration of particles in our simulations consists of a collection of independent one-dimensional lattice systems, all governed by the same transition rule. We mention here that the lattice gas measurements carried out for all the examples in this article consist of ensemble averages; we have not used coarse-graining on a single lattice system. Each system is initialized stochastically, namely by placing particles site-by-site with probabilities determined by the initial velocity profile that we want to simulate:

$$P_j^0 = \frac{1}{2}\left(1 - \frac{v_j^0}{V}\right)$$

For our examples we have run several (typically 100) simultaneous one-dimensional lattice experiments, measuring particle count on each column to produce the lattice measurements shown in the figures.

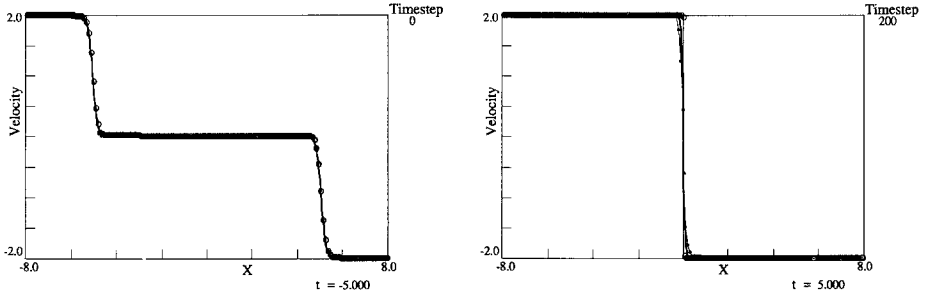

Fig. 1. Shock formation: exact solution (heavier solid curve), automaton measurements (*), and finite-difference results (○). $\mu = 1/10$, $\alpha = 1$ (deterministic dynamics). Initial conditions were specially prepared so that fluctuations in particle concentration are minimized for each of the 1D lattice systems. The greater the fluctuation of particle number in each system of the initial configuration, the less sharp is the shock in the lattice equilibrium.

The first simple example is shown in Fig. 1: standing shock formation from nonequilibrium initial conditions. Included are the exact solution, automaton measurements, and the results of numerical iteration (10), that is, the results of the finite-difference scheme subject to conditions (12). The exact solution for this example is already near its equilibrium profile at $t=0$; to start the simulation well outside equilibrium, we have simply chosen an earlier initial time, specifically, $t=-5$. Initial conditions were specially prepared so that fluctuations in particle concentration in each 1D lattice system were minimized, yielding a sharp shock in the lattice equilibrium. This is in contrast with Fig. 5, showing the same example but initialized without regard to fluctuations; for the moment notice simply that in the final time we see a wider shock in the lattice equilibrium.

Remark now that if finite-difference equation (11) with discretization (12) gives a poor approximation to Burgers' equation, then even when this master equation furnishes a perfect statistical description of the particle distribution, the lattice gas simulation will be inadequate. Thus we consider in the next section the behavior of the solution of the finite-difference scheme.

4. MONOTONICITY AND THE ENTROPY CONDITION

Consider Figs. 2 and 3. The test problem is the same in both cases: an initial discontinuity which disperses in a rarefaction wave. The only implementational difference between the lattice simulations for the two examples is the parameter α: $\alpha=1$ in Fig. 2 and $\alpha=1/2$ in Fig. 3. We can explain the difference in behavior for the two cases by considering the property of monotonicity of the numerical scheme simulated by the lattice

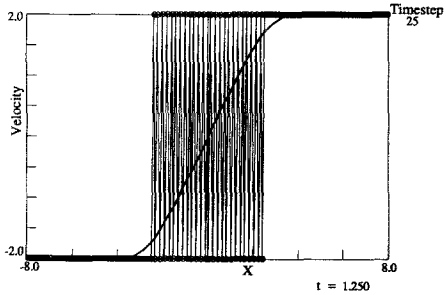

Fig. 2. Rarefaction wave: exact solution (heavier solid curve), automaton measurements (*), and finite-difference results (○). $\mu=1/10$, $\alpha=1$ (deterministic dynamics). Same initial conditions, $t=0$, as Fig. 3. Automaton measurements are exactly superimposed on finite-difference results. Not a monotone scheme.

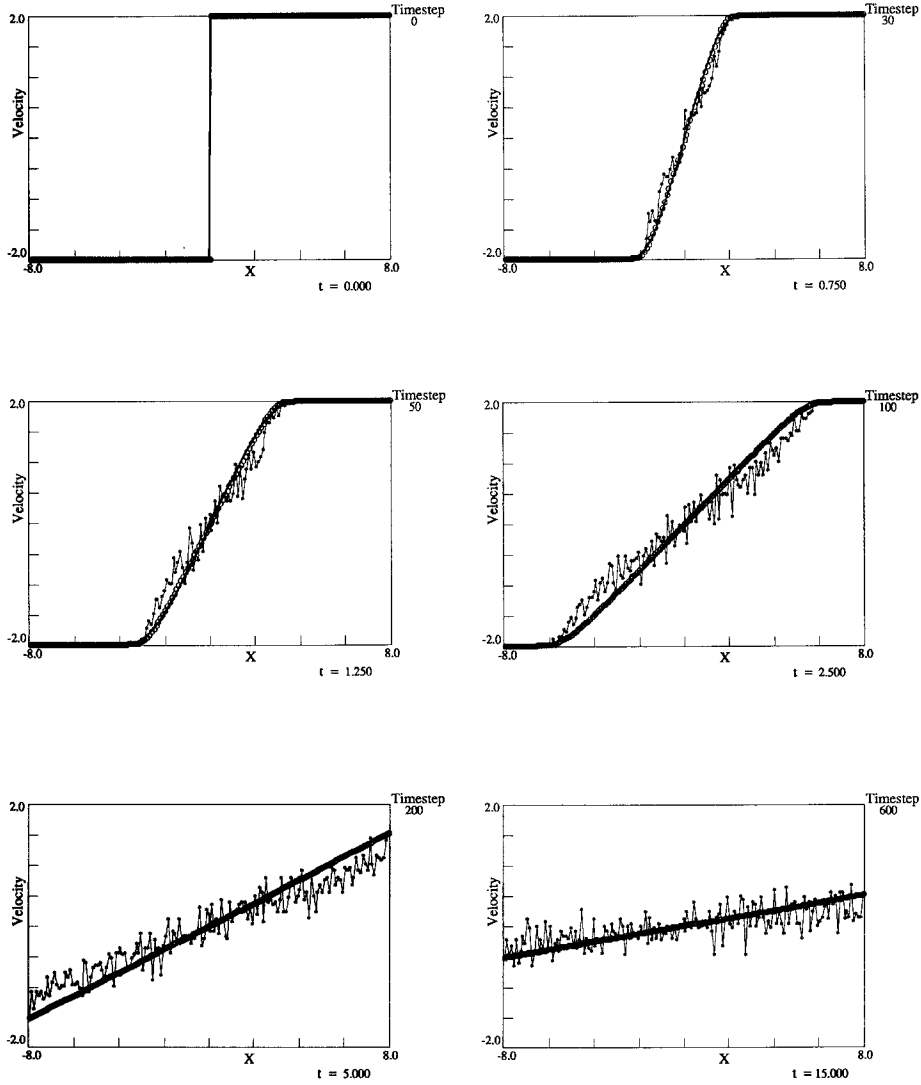

Fig. 3. Rarefaction wave: exact solution (heavier solid curve), automaton measurements (*), and finite-difference results (○). $\mu = 1/10$, $\alpha = 1/2$. A monotone scheme.

gas. Consider the numerical iteration defined by the balance equation (10) and written in the form $v_j^{n+1} = H(v_{j-1}^n, v_j^n, v_{j+1}^n)$:

$$v_j^{n+1} = (1-\alpha)\, v_j^n + \frac{\alpha}{2}(v_{j+1}^n + v_{j-1}^n) - \frac{\alpha}{2V} v_j^n (v_{j+1}^n - v_{j-1}^n) \tag{13}$$

Such a numerical scheme is monotone if $\partial H/\partial v_k \geqslant 0$, $k = j-1, j, j+1$, for all j in the interior of the configuration.[10] For the numerical scheme given in (13), the requirements on v for monotonicity are thus

$$\begin{cases} -V \leqslant v_j^n \leqslant V \\ v_{j-1}^n - v_{j+1}^n \geqslant 2V\left(\dfrac{\alpha-1}{\alpha}\right) \end{cases} \tag{14}$$

everywhere on the configuration. Notice that since P is a probability and $v = (-2P+1)\, V$, the first two conditions are automatically true. As for the third, we consider separately the two cases $\alpha = 1$ and $0 < \alpha < 1$.

When $\alpha = 1$, the third condition for the monotonicity of the numerical scheme is satisfied whenever the solution is a nonincreasing function of x. Since a monotone scheme is monotonicity-preserving, once this condition is satisfied everywhere on the configuration, under iteration (13), it will continue to hold. Thus, if the initial conditions of a simulation satisfy (14), then the iteration is and remains monotone. This corresponds to an initial profile of velocities in which the faster fluid particles are to the left and overtake the slower moving particles, or those with negative velocity, to the right. These are just the conditions under which the solution forms a shock (Fig. 1).

Conversely, if conditions (14) are violated in the initial configuration, then we do not have a monotone scheme. In fact, if this is the case everywhere on the configuration, i.e., if $v_{j-1}^n < v_{j+1}^n$ everywhere, then under the effects of iteration (13), this will always be the case. This corresponds to an initial profile of slower particles on the left and increasingly faster particles to the right, in which case the solution exhibits a rarefaction or expansion wave. In this situation we are assured that the above scheme will never be monotone. Figure 2 shows such an example; the numerical scheme is not convergent.

Now consider the case $0 < \alpha < 1$. Notice that if $\alpha \leqslant 1/2$, then $(\alpha-1)/\alpha \leqslant -1$, and the third requirement for monotonicity is automatically satisfied since $v_{j-1}^n - v_{j+1}^n \geqslant -2V$ is always true. Thus, if $\alpha \leqslant 1/2$, then for *any* initial velocity distribution, the resulting numerical scheme is guaranteed to be monotone. Figure 3 shows the rarefaction wave example of Fig. 2, only now with $\alpha = 1/2$.

For the sake of clarifying the importance of monotonicity in this numerical scheme, we consider the inviscid, hyperbolic Burgers' equation [Eq. (1) with $\mu = 0$] in conservation form

$$u_t + f_x = 0 \tag{15}$$

with flux function $f(u) = u^2/2$. The solutions of this equation exhibit features different from those of the viscid, parabolic equation ($\mu \neq 0$). For example, in the viscid equation, shocks are smoothed out by the effect of dissipation, whereas in the inviscid equation, shocks are true discontinuities and piecewise continuous weak solutions are admitted. Constrained to respect the conservation law of Eq. (15), any such weak solution must satisfy the Rankine–Hugoniot jump condition across a discontinuity:

$$s = \frac{u_l + u_r}{2} \tag{16}$$

where s is the speed of propagation of the discontinuity and u_l and u_r are the velocities to the left and right of the discontinuity, respectively.

Another difference between the two equations lies in the unicity of the solutions. The solution of the viscid equation is uniquely determined by initial conditions, and the unique solution is considered physically relevant. On the other hand, weak solutions of the inviscid equation, even those respecting the Rankine–Hugoniot condition, are neither necessarily unique nor physical. For given initial conditions, there *is* a unique solution considered physically relevant, but there can be other, spurious solutions. An additional condition is imposed in order to distinguish the physical one from the others.[3,10,11]

The principle applied is that any physical solution of the inviscid equation is presumed to be "near" the solution of the viscid equation with some (small) dissipation. More precisely, a physical solution of the inviscid equation must be the limit as ε tends to zero of solutions of equations of the form

$$u_t + f_x(u) = \varepsilon(\beta u_x)_x \tag{17}$$

For such a solution the following inequality has been shown to hold at a (shock) discontinuity:

$$\frac{f(u) - f(u_l)}{u - u_l} \geqslant \frac{f(u) - f(u_r)}{u - u_r} \tag{18}$$

where u is any value between u_l and u_r. In addition, the weak solution of Eq. (15) which satisfies condition (18) is unique.[11,12] For Burgers' equa-

tion, the condition (18) which distinguishes the physical solution from the others is that

$$u_l \geqslant u_r \tag{19}$$

at any discontinuity of the solution. Thus physical solutions must decrease across shocks (discontinuities); increasing solutions must be shock-free (continuous).

An analogous relation between the velocities on either side of a shock in a perfect gas follows from the second law of thermodynamics: entropy cannot decrease in adiabatic flow and this can be used to demonstrate that, across a normal shock wave, velocity is constrained to decrease from supersonic to subsonic.[13] By analogy, then, inequality (19) above is known as an *entropy condition.*

Not surprisingly, a numerical method for approximating the solution of Burgers' equation must also take into account the physics modeled by the continuous equation. For instance, a difference scheme for the inviscid Burgers' equation which cannot itself be written in conservation form can converge to a function which is *not* a weak solution of the original equation, because it is not constrained to respect the Rankine–Hugoniot conditions.[10] A k-step finite-difference approximation to (15) is in conservation form if it can be written as

$$u_j^{n+1} = u_j^n - \lambda[g(u_{j-k+1}^n, u_{j-k+2}^n, \ldots, u_{j+k}^n) - g(u_{j-k}^n, u_{j-k+1}^n, \ldots, u_{j+k-1}^n)] \tag{20}$$

where $\lambda = \Delta t/\Delta x$ is a constant and g is the numerical flux; it is *consistent* with the original conservation equation if $g(u, \ldots, u) = f(u)$.[11] Beyond this, a numerical scheme consistent with Eq. (15) but which does not itself respect the entropy condition risks converging to one of the spurious, nonphysical weak solutions of the equation.

Now the reason for the foregoing consideration of the inviscid equation should become clear when we remark that the finite-difference scheme approximation for the viscid Burgers' equation, Eq. (11) under conditions (12), is consistent with the *inviscid* equation (15). To see this, notice that the scheme (11) can be written in conservation form

$$u_j^{n+1} = u_j^n - \lambda[g(u_j^n, u_{j+1}^n) - g(u_{j-1}^n, u_j^n)] \tag{21}$$

with $\lambda = \Delta t/\Delta x = \alpha/V$ constant and numerical flux $g(a, b) = (\mu/\Delta x)(-b + a) + ab/2$. Since $g(u, u) = u^2/2 = f(u)$, this scheme is consistent with the inviscid Burgers' equation. That is, the continuous limit of the difference scheme (11) as Δx, $\Delta t \to 0$, under conditions (12) with α fixed, is the inviscid Burgers' equation.

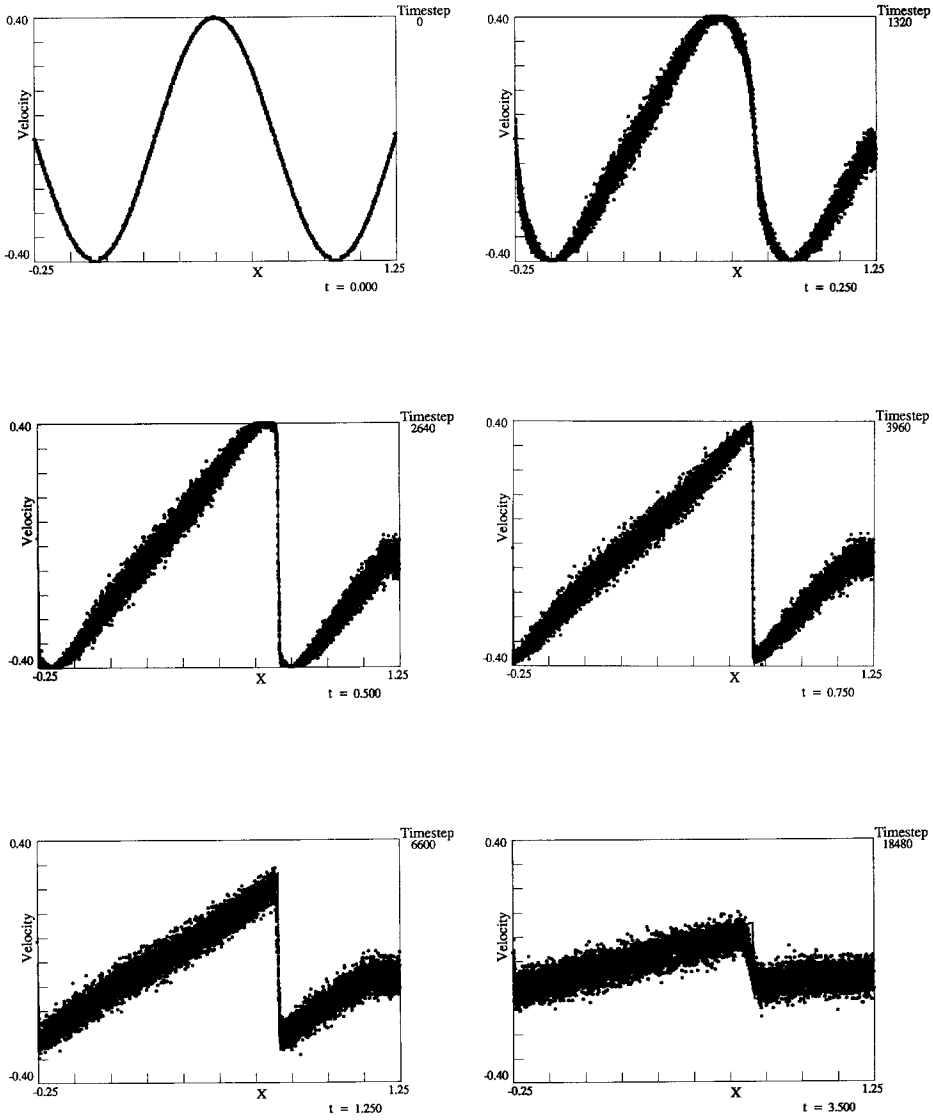

Fig. 4. Periodic initial conditions: finite-difference results (solid curve) and automaton measurements (*). $\mu = 3 \times 10^{-5}$, $\alpha = 1/2$. The evolution of the system illustrates shock formation and rarefaction wave dissipation. Fluctuations somewhat controlled in initial conditions: some shock widening.

Thus the balance equation of the lattice gas model, derived as an approximation to the viscid Burgers' equation, is actually consistent with the inviscid Burgers' equation. This is not necessarily a problem: the physical solution of the inviscid equation is "near" the solution of the equation with viscosity, and one may expect a single numerical solution to describe relatively well the solutions of both equations. However, if the lattice solution does not respect the entropy condition, it may reproduce a first-order approximation to a nonphysical solution of the inviscid equation, smoothed somewhat by the second-order dissipation term, and simply miss completely the solution of the viscous equation.

Now, back to monotonicity and the behavior shown in Fig. 3. A monotone scheme in one dimension necessarily respects the entropy condition and, if convergent, converges to the physical solution.[10,11] Recall that with the probability α as parameter in the lattice model as described above, when $\alpha \leqslant 1/2$, the master equation of the lattice gas corresponds to a monotone scheme, and we can expect the lattice results to be near the solution of the viscous equation.

In Fig. 4 we see another lattice gas simulation with $\alpha = 1/2$, in an example with periodic initial conditions. The evolution of the system illustrates shock formation and rarefaction wave dissipation.

5. CAPTURING A MOVING FRONT

In Section 4 we found conditions under which Eq. (10) defines a monotone scheme, implying entropic solutions. Up to this point we have assumed that our master equations (8)–(10) adequately describe the behavior of the particle system as observed in the column-by-column measurements of the lattice gas particle density. Judging by the example in Fig. 4 of rarefaction and shock formation *without* propagation, this assumption appears to be justified. Consider now Fig. 5, an example of front propagation evolving to a standing front. The fact of the matter is that the numerical solution of (10) does adequately represent the solution of Burgers' equation in this example with $\mu = 1/10$, but the profile of v calculated from the actual particle distribution does not. Evidently, Eq. (8) does not always correctly describe the quantitative behavior of the particle density.

As for the particle system itself, notice that in the example of Fig. 5, for which the lattice dynamics was defined by $\alpha = 1$, the lattice measurements exhibit the appropriate shock features *except* for the speed of shock propagation. The scaling used in our model is imposed by the conditions (12), which imply, for fixed α, that in the continuum limit $\Delta t/\Delta x$ remains fixed and $\Delta x^2/\Delta t \to 0$. This is not a scaling limit which captures diffusion or

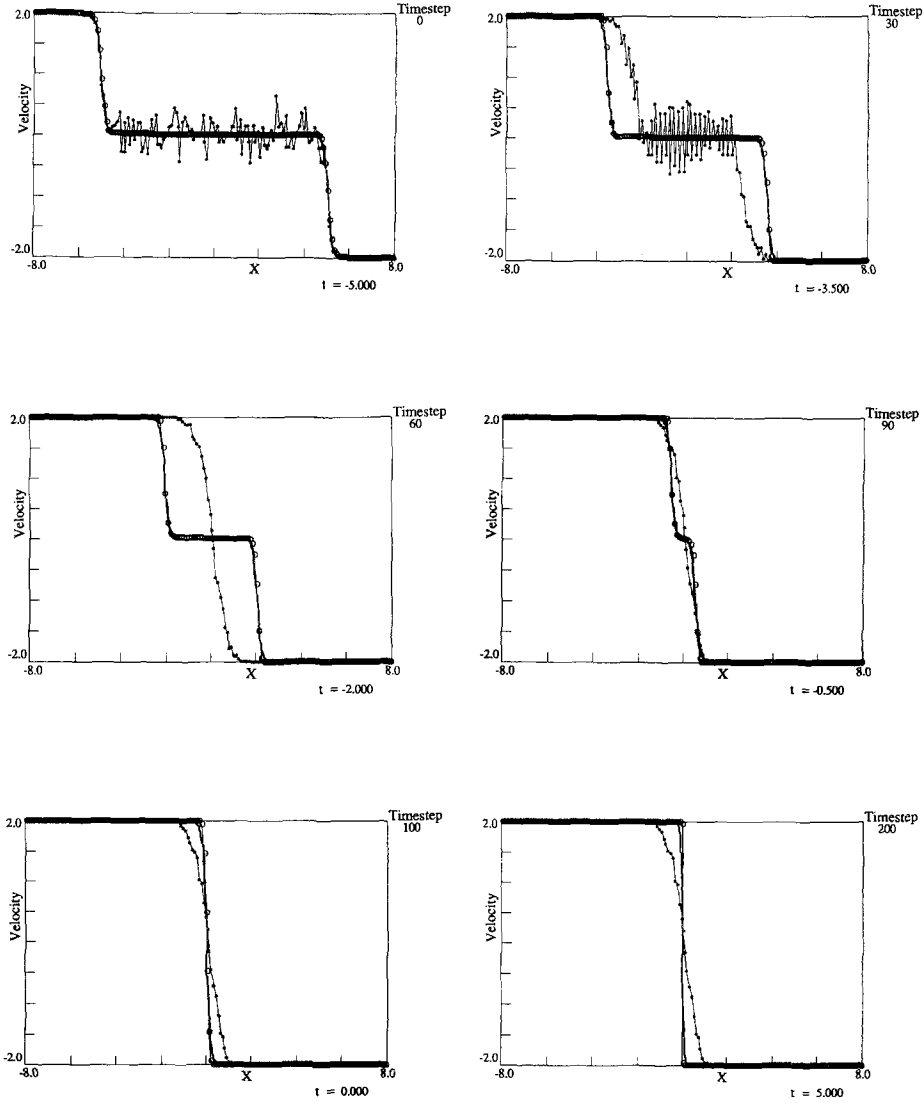

Fig. 5. Shock propagation: exact solution (heavier solid curve), automaton measurements (*), and finite-difference results (○). $\mu = 1/10$, $\alpha = 1$ (deterministic dynamics). The lattice measurements exhibit the appropriate shock features *except* for the speed of shock propagation. Fluctuations not controlled in initial conditions: shock widening.

its effects on front propagation in the model. We might consider another scaling where $\Delta t/\Delta x \to 0$ and $\Delta x^2/\Delta t$ remains constant, in which case diffusion should be captured. To do so, we must adjust our scaling to be compatible with this diffusive limit and yet continue to respect conditions (12), fundamental to our simulation. This is possible if, in approaching the continuum, we consider α variable.[14] Remark that conditions (12) imply that $\mu = \mathcal{O}(\Delta x)$. If we let $\alpha = \mu$, then we indeed find ourselves with the scaling in which $\Delta t/\Delta x \to 0$ and $\Delta x^2/\Delta t$ is fixed, *and* we respect conditions (12) so important to our model. This is then the scale on which the particle system should be able to exhibit diffusive behavior.

It is not *a priori* clear which values of α are sufficiently small so that the lattice gas captures the effect of dissipation consistent with the solutions of Burgers' equation and of the master equation (10). For the initial conditions of Fig. 5, setting $\alpha = \mu = 1$ yields the same behavior as in Fig. 5, meaning that these values are so large that convection incorrectly dominates the model. Figure 6 shows the same example but with $\alpha = \mu = 1/10$, and Fig. 7 shows an example of front propagation with $\alpha = \mu = 1/100$. The scaling appears adequate in these two cases.

Not surprisingly, the "sufficiently" small values of α are those which also ensure that the master equation (8) yields a quantitatively good description of the lattice particle distribution. Transition probabilities (7) used to derive Eq. (8) were approximated using the assumption that occupation probabilities at neighboring sites are decorrelated. The smaller the parameter α, the smaller the effect of this approximation and the closer the solution of (10) to the profile of v calculated from the actual particle density.

Another feature worth noticing in the figures is the shock width in the lattice gas simulation. A shock in an individual lattice system can be microscopically sharp, but each such system, initialized stochastically according to the same probability profile, will have its own shock position determined by the initial particle placement. The particle distribution, averaged over several lattice systems, will manifest a shock width dependent on the individual shock positions. In general, when the configurations of particles are initialized stochastically, there are resultant fluctuations around the desired initial velocity profile. A shock seems to be a point of accumulation of the effect of these initial particle fluctuations, apparently due to the unidirectional nature of the dynamics. In closed systems, the fluctuation in total number of particles initially placed in each lattice system determines the shock width. For these closed systems, assuming an initial multinomial probability distribution on N lattice sites, the relative shock width diminishes in the hydrodynamic limit as $N^{-1/2}$. Figure 5, in which fluctuations were not controlled in the initial conditions, exhibits

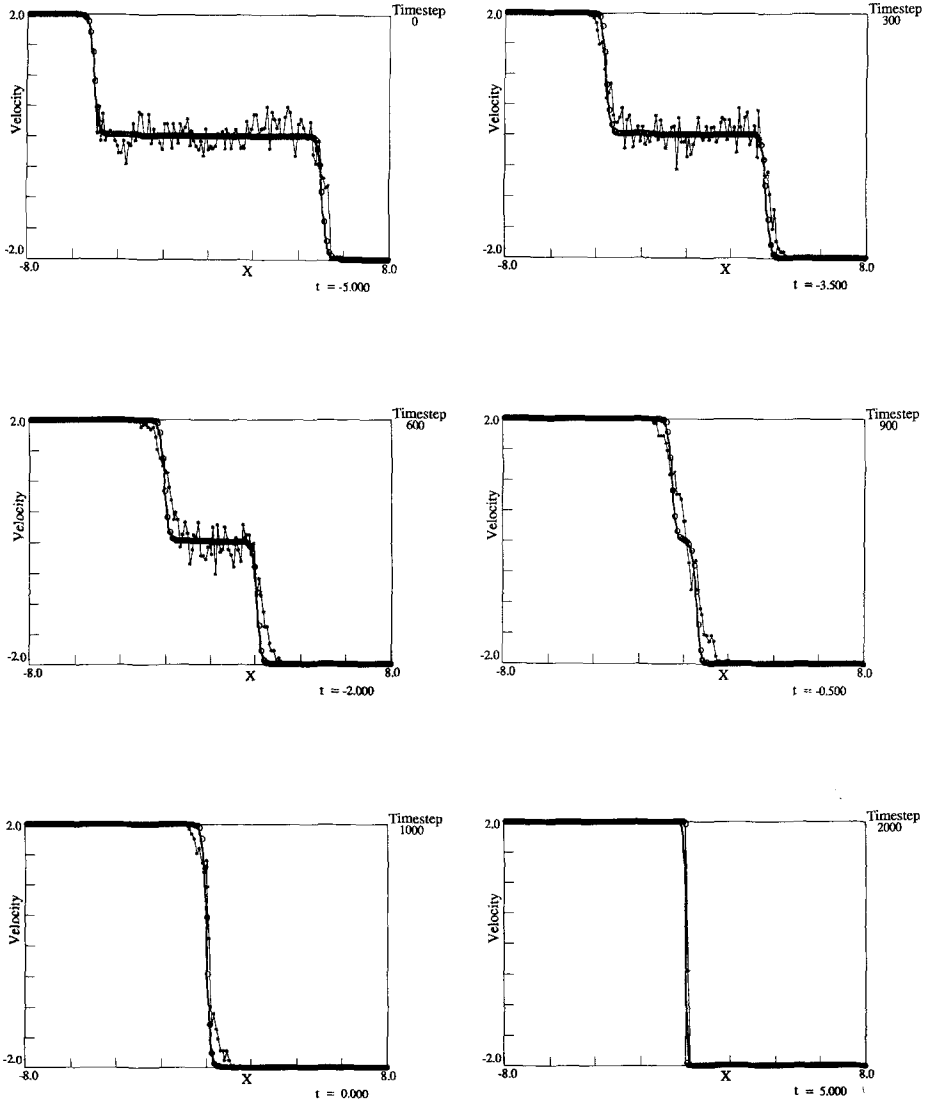

Fig. 6. Shock formation: exact solution (heavier solid curve), automaton measurements (*), and finite-difference results (○). $\mu = 1/10$, $\alpha = 1/10$. The lattice measurements exhibit the appropriate speed of shock propagation. Initial conditions which force an identical number of particles in each of the 100 1D lattice systems: the shock is sharp.

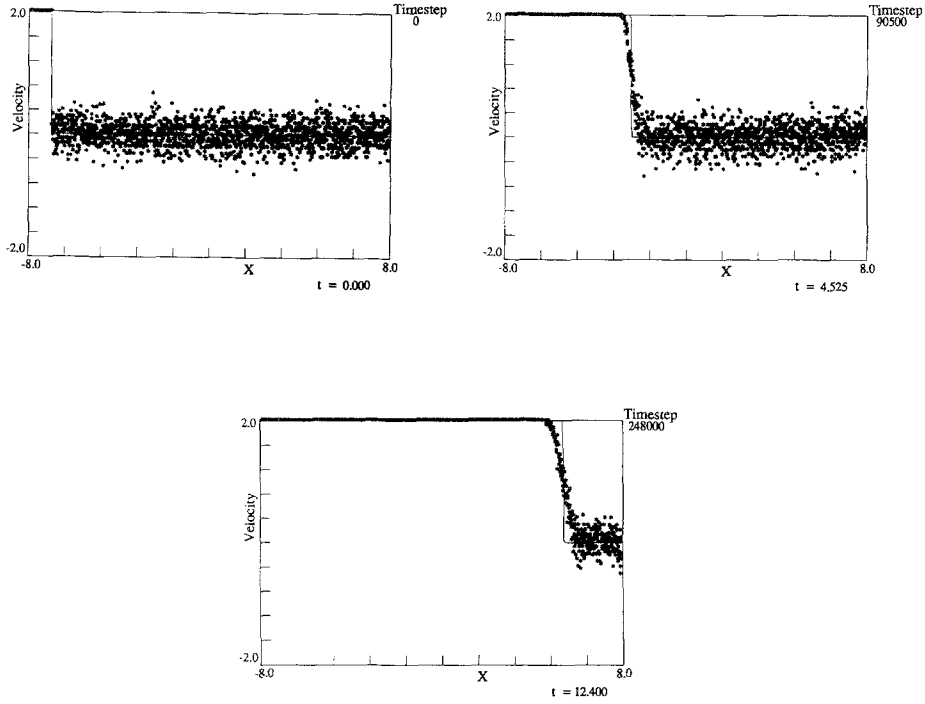

Fig. 7. Front propagation: finite-difference solution (solid curve) and automaton measurements (*). $\mu = 1/100$, $\alpha = 1/100$. The lattice measurements exhibit the appropriate speed of shock propagation. Fluctuations not controlled in initial conditions: some shock widening.

shock widening. This is in contrast to Figs. 1 and 6, in which initial fluctuations were minimized. The cumulative effect of the initial fluctuations on the shock width is also seen in Figs. 4 and 7.

6. CONCLUSION

A lattice model, a simplified universe consisting of a large number of particles and governed by its own extremely simple laws, can capture the macroscopic properties observed in a physical system and this without necessarily requiring the detailed realism of the dynamics. This is not completely surprising given that, in general for both lattice *and* physical systems, the global characteristics actually observed are the composite effect of an enormous number of elementary processes, whose essential

natures are completely hidden by the reducing effect of the law of large numbers.

We have considered in this article a stochastic lattice gas model for Burgers' equation, with a simple approximation of the master equation. The behavior of the model has been illustrated in several examples encompassing the various characteristics of solutions of Burgers' equation, including shocks and rarefaction waves. Under appropriate conditions on the parameter α, which governs the lattice gas dynamics, μ, the constant of diffusion in the equation, and the discretizations Δx and Δt, this master equation is equivalent to a finite-difference discretization of Burgers' equation. Questions of convergence to the right (physical) solution have been investigated: a condition on α has been found which guarantees that solutions of the approximate master equation respect an entropy condition. An additional condition on α relative to μ has been observed to yield the scaling appropriate for front propagation in the lattice simulation. Under this same condition the description of the particle system furnished by the approximate master equation is refined.

This study of a lattice model for Burgers' equation has been intended to clarify the sort of considerations generally necessary in the construction and evaluation of lattice models for given PDEs. We can expect that with more complicated models of more complex equations, such investigations will become all the more necessary and intricate.

ACKNOWLEDGMENTS

The authors would like to thank Charles Edouard Pfister for helpful conversations during which we benefitted from his experience and advice.

This work has been partly sponsored by a grant from the Fond National Swisse and was accomplished in part at the CNLS, Los Alamos National Laboratory.

REFERENCES

1. J. M. Burgers, Mathematical examples illustrating relations occurring in the theory of turbulent fluid motion, *Trans. R. Neth. Acad. Sci. Amsterdam* **17**:1 (1939).
2. J. Smoller, *Shock Waves and Reaction-Diffusion Equations* (Springer-Verlag, New York, 1983).
3. D. Euvrard, *Résolution Numérique des Equations aux Dérivées Partielles* (Masson, Paris, 1990).
4. E. R. Benton and G. W. Platzman, A table of solutions of the one-dimensional Burgers' equation, *Q. Appl. Math.* **xxx**(2):195 (1972).
5. W. Feller, *An Introduction to Probability Theory and Its Applications* (Wiley, New York, 1964).

6. L. Brieger and E. Bonomi, A stochastic cellular automaton simulation of the non-linear diffusion equation, *Physica D* **47**:159 (1991).
7. L. Brieger and E. Bonomi, A stochastic cellular automaton model of nonlinear diffusion and diffusion with reaction, *J. Comp. Phys.* **94**(2):467 (1991).
8. B. M. Boghosian and C. D. Levermore, A cellular automaton for Burgers' equation, *Complex Systems* **1** (1987).
9. J. L. Lions, *Cours d'Analyse Numérique* (Ecole Polytechnique, Paris, 1984).
10. E. Godlewski and P.-A. Raviart, *Hyperbolic Systems of Conservation Laws* (Ellipses, Paris, 1991).
11. A. Harten, J. M. Hyman, and P. D. Lax, On finite difference approximations and entropy conditions for shocks, *Commun. Pure Appl. Math.* **xxix**:297 (1976).
12. O. A. Oleinik, Discontinuous solutions of nonlinear differential equations, *Uspekhi Mat. Nauk* **12**:3 (1957) (*Am. Math. Soc. Transl. Ser. 2* **26**:95).
13. H. W. Liepmann and A. Roshko, *Elements of Gas Dynamics* (Wiley, New York, 1957).
14. J. L. Lebowitz, E. Orlandi, and E. Presutti, Convergence of stochastic cellular automaton to Burgers' equation: Fluctuations and stability, *Physica D* **33**:165 (1988).